Precise Scanner of Magnetic Field Distribution

Martin Vítek, Martin Juřík and František Mach

***Abstract*— The magnetic field scanner hardware together with basic operation parameters are discussed. The proposed multi-sensor scanner has a base resolution of 10 px × 10 px. By micropositioning across the area 50 mm × 50 mm, it is possible to achieve resolution up to 10 000 px × 10 000 px with spatial resolution up to 5 µm. As a result, precise distribution of the magnetic field around an examined object with complex magnetization is obtained.**

***Index Terms*— Sensor array, measuring magnetic field, magnetic scanner.**

I. Introduction and Motivation

The development of magnetically guided meso-scale and micro-scale robots has been transformed from a rigid design to soft or flexible structures with programmable magnetization [1] [2]. Whereas external magnetic field used for robot actuation is well described, the internal magnetization of robot body can be subject of uncertainty such as the material non-uniformity, manufacturing tolerances, stability or non-linearity of material parameters [3]. Post-production mapping of the robot's magnetization allows to determine the real distribution of generated magnetic field and then calibrate mathematical models of the robot.

There are several research groups that deal with magnetic fields mapping, but most of them use either only one sensor [4] or static sensor array [5]. We combined both these options to obtain high resolution and fast scanning. The complete hardware of our scanner is described in the following section. Measurements of the sensor's characteristics (Section III) are further discussed and illustrative scans are shown in Section IV.

II. Hardware and Software Description

The magnetic scanner consists of three parts. The first part is a measuring device, the second part is a micropositioning device and the third part is PC software.

The measuring device is based on sensor LSM303AGR, which includes a triple-axis magnetometer, triple-axis accelerometer, and thermometer in package LGA-12 with dimensions of 2 mm × 2 mm. The sensor characteristics provided by the manufacturer are summarized in Table I. The sensor communicates via I^2C or SPI bus. The magnetometer is based on the AMR (Anisotropic Magnetoresistance) technology, with set and reset coils for eliminating the offset hysteresis.

This research has been supported by the Ministry of Education, Youth and Sports of the Czech Republic under the RICE New Technologies and Concepts for Smart Industrial Systems, project No. LO1607 and by the University of West Bohemia under the project SGS-2018-043.

Authors are with the Faculty of Electrical Engineering, University of West Bohemia, 301 00 Pilsen, Czech Republic {martinv, mjurik, fmach}@kte.zcu.cz

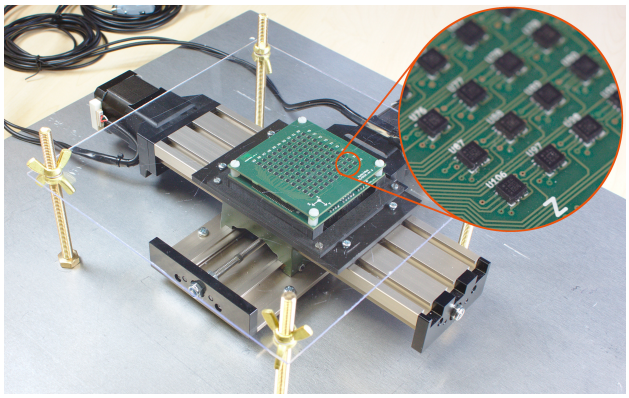

Fig. 1. Magnetic scanner with measuring device with 100 triple-axis magnetometers LSM303AGR and $x-y$ table mounted on an aluminium base.

To speed up scanning of the magnetic field, 100 sensors were used in the matrix 10 by 10 with a spacing of 5 mm. The total area is, therefore, 45 mm × 45 mm and scanning speed is 100× higher than with single sensor.

The sensors communicate with the microcontroller over the SPI bus. The magnetometer and accelerometer are separate sensors in one package, so that each of them has separate CS (chip select) line. This means that 200 CS lines are needed to address all the sensors. To minimize the pin count of the microcontroller, only four accelerometers were connected. Eight 4 to 16 demultiplexers CD75HC154M were used to connect the resulting 104 CS lines to 12 pins of the microcontroller.

TABLE I
LSM303AGR magnetic characteristics

Dynamic range	±4.9152 mT
Sensitivity	150 nT/LSB
Offset	±6 µT
Output data rate	100 Hz
RMS noise	300 nT
Sensitivity change	±0.03 %/°C
Offset change	±30 nT/°C

The device is controlled by an ARM Cortex M0+ microcontroller ATSAMD21G17A with 128 kB FLASH and 16 kB RAM, running at 48 MHz. Communication with the computer is possible by USB with a virtual serial port, over embedded UART to USB converter FT231XS, at 3 MBd.

The measuring device is split into two 4-layer PCBs. The first PCB is for measuring and contains only sensors with decoupling capacitors. The second one is assembled with controlling microcontroller and communication. This arrangement allows possible exchange of one PCB with reuse of another one in the future.

The micro-positioning device is built on $x-y$ table KT 70 CNC-ready. It's characteristics are summarized in Table II. The stepper motors of the table are controlled with two stepper drivers HY-DIV168N-3.5A and Arduino Uno. The overall construction of this device is built as robust as possible, with the use of mainly non-ferromagnetic materials. Unfortunately, threaded rods of the $x-y$ table are made of steel and also stators of the stepper motors are made of ferromagnetic metal sheets.

TABLE II
KT 70 CNC-READY CHARACTERISTICS

Material	Al
Travel x-axis	150 mm
Travel y-axis	70 mm
Step	5 µm

The PC software is programmed in C++17 using the server-client architecture. The server side communicates with the measuring and positioning device and controls the measurement process. The user interface is made as a web page communicating with the server via WebSockets. It is possible to run this software both on Linux and Windows.

The scanner can be used in several modes. The live mode shows the magnetic field live with a 10 px × 10 px resolution. When measuring in time, the magnetic data are captured over the defined time period in the 10 px × 10 px resolution. Detailed measurement combines saving data and positioning of the scanner to create a detailed scan of a 50 mm × 50 mm area with a resolution up to 10 000 px × 10 000 px with a position step equal to 5 µm. Pixel means one point in space, where three components of the magnetic flux density vector were measured.

III. Measurements of Magnetic Sensors

Several measurements were performed to characterize the sensor's magnetometer performance. Some of the measurements were done in magnetically shielded rooms to minimize the magnetic noise from environment. Linearity and noise were measured in an electron microscope lab and time drift was measured in an EMC chamber.

A. Linearity

Linearity was obtained by measuring the magnetic field of an air-core coil placed on measuring device. For each current level through the coil, magnetic field over 100 samples (2 s) was measured and the mean value was plotted as can be seen in Fig. 2.

B. Amplitude Frequency Response

To get the maximum frequency of the magnetic field which can be measured, the amplitude frequency response was measured using an air-core coil excited with a sine wave from a signal generator. Magnetometer's ODR (Output Data Rate) was set to 50 Hz. The internal digital low-pass filter was set with values of ODR/2 and ODR/4. Between the values measured by different low-pass filters are not any significant differences as shown in Fig. 3, probably due to enabled offset cancellation.

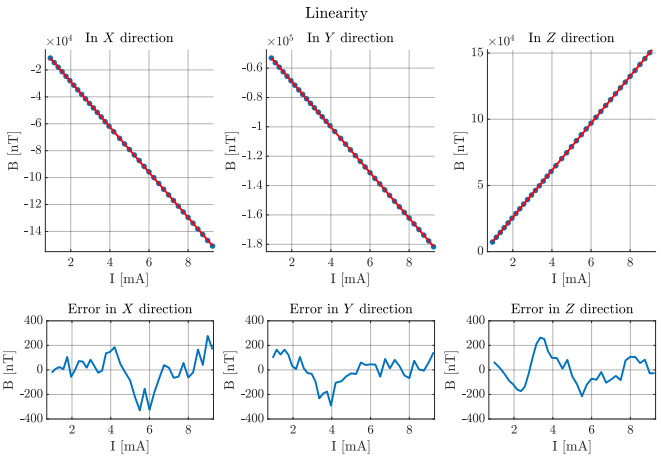

Fig. 2. On top graphs, circles represent measured magnetic flux density B and red line is linear function fitted to measured data. The error between measured data and fitted function is shown on bottom graphs. Columns represent each axis of the magnetometer separately.

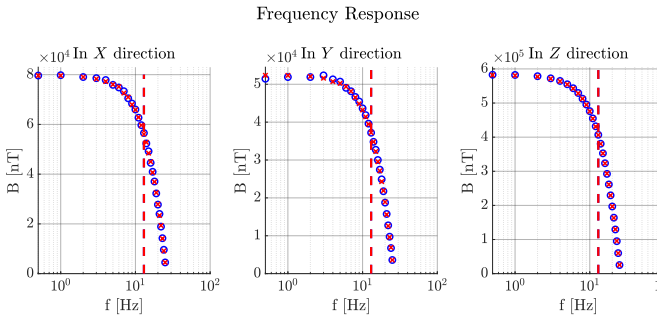

Fig. 3. Blue circles and red crosses represent measured magnetic flux density B with filter sets to ODR/2 and ODR/4, respectively. The dashed line shows $f_{\max}$, based on drop of amplitude by 3 dB (0.71 of $B_{0.5\,\mathrm{Hz}}$).

C. Noise

To analyse the noise of magnetometers, 3 000 samples (60 s) were taken of surrounding magnetic field in the magnetically shielded room. Standard deviations of all magnetometers are shown in Fig. 4.

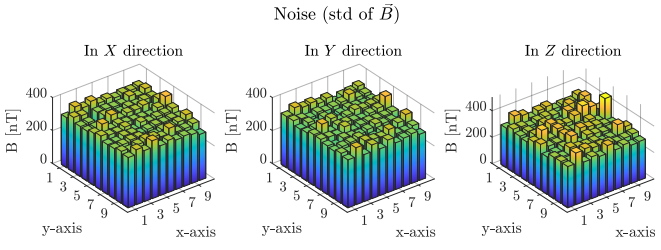

Fig. 4. Standard deviations of measured magnetic flux density. Axes X and Y determines position of sensor in matrix, Z axis shows standard deviation.

D. Time Drift

Time drift was determined by taking 200 000 samples (≈1 h) of the magnetic field in the EMC chamber. Figure 5 shows time drift as the difference between the measured value and average value from the beginning of the measurement.

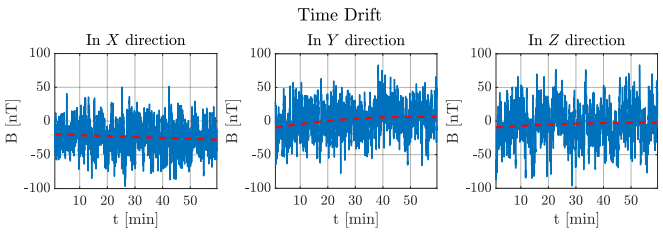

Fig. 5. Blue line is difference between measured magnetic flux density B and average value from beginning of measurement in time. Red dashed line is second order polynomial fitted to measured data.

E. Temperature Stability

To analyse the temperature stability, measuring device was placed into a laboratory furnace, heated from 22 °C to 85 °C and magnetic field of surrounding space was recorded. At each temperature, 250 samples (5 s) were taken. Change of the magnetic flux density with temperature and error between values measured at 30 °C and 85 °C are shown in Fig. 6.

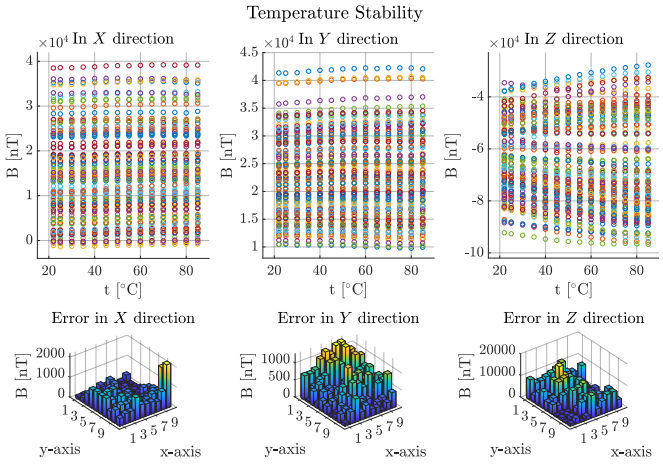

Fig. 6. Dependence of magnetic flux density B on temperature is represented by top graphs for each axis and each magnetometer. On bottom graphs, X and Y axes determines the position of sensor in matrix, Z axis shows error between 30 °C and 85 °C.

IV. Illustrative Scans

Several pictures are presented to show the capabilities of the presented scanner. First, the maximal spatial resolution of 5 µm is shown in Fig. 7. Second, two captured datasets are shown in Fig. 8. The left part shows the magnetic field around the permanent magnet in base resolution, without moving the scanner. The right part shows the array of 100 permanent magnets scanned with scanner moving 20 steps by 250 µm along x and y axes. Each peak represents the field around one magnet. The difference between magnets, due to manufacturing tolerances, is clearly visible.

V. Conclusion

From all the above results, it is possible to conclude that with the created scanner, the errors can be almost neglected in the standard measurement process. For measuring the static magnetic field at room temperature, the parameters are as follows:

- linearity error is approx. ±200 nT,
- standard deviation of noise is approx. 350 nT,
- time drift is almost not present,
- spatial resolution is up to 5 µm.

Currently, we are using the magnetic sensor array (measuring device) for non-visual tracking of our rigid magnetic minirobots in the working area. We are planning to use the presented magnetic scanner for calibrating the mathematical model of our minirobots [6] for reducing tracking uncertainty. Also post-production mapping of our magnetic soft-bodied robots is a future goal.

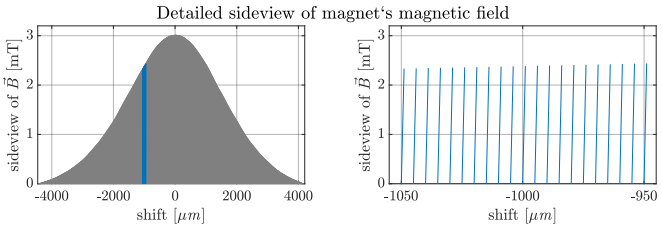

Fig. 7. Detailed orthogonal side view of scanned cubic magnet of size of 1 mm × 1 mm × 1 mm with measurement step equal to 5 µm. Left part shows complete distribution, right part depicts marked area in detail.

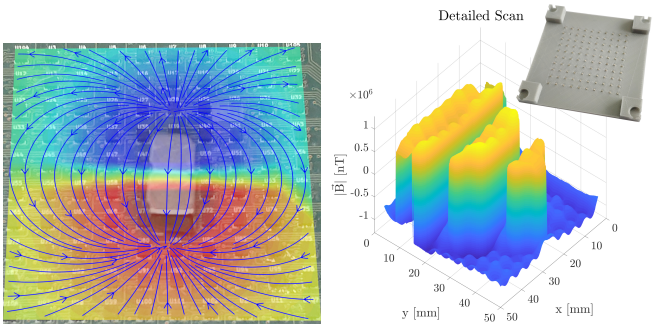

Fig. 8. Left part shows measured magnetic field of neodymium magnet in resolution 10 px × 10 px. Colour map corresponds to amplitude of magnetic flux density and blue lines illustrate force lines. Right part shows detailed scan of 10 × 10 matrix of small neodymium magnets (top right corner) with resolution 200 px × 200 px (step 250 µm, scan time ≈90 s).

References

[1] XU, Tianqi, et al. 'Millimeter-scale flexible robots with programmable three-dimensional magnetization and motions'. Science Robotics, 2019, 4.29:4494.

[2] HU, Wenqi, et al. 'Small-scale soft-bodied robot with multimodal locomotion'. Nature, 2018, 554.7690:81.

[3] KIM, Yoonho, et al. 'Printing ferromagnetic domains for untethered fast-transforming soft materials'. Nature, 2018, 558.7709:274.

[4] BERGSMA, F., et al. 'A High Precision 3D Magnetic Field Scanner for Small to Medium Size Magnets'. IEEE Transactions on Applied Superconductivity, 26:4, 2016.

[5] RAHMAWATI, Dien, et al. 'Magnetic Imaging System Based on HMC5883L Sensor Array'. International Conference on Instrumentation, Communications, Information Technology, and Biomedical Engineering (ICICI-BME), 2017.

[6] JUŘÍK, M., et al. 'Positioning Uncertainty Reduction of Magnetically Guided Actuation on Planar Surfaces'. IEEE International Conference on Robotics and Automation (ICRA), 2019.